



# High performance hybrid supercapacitors using granule $\text{Li}_4\text{Ti}_5\text{O}_{12}$ /Carbon nanotube anode

Byung-Gwan Lee <sup>a, c, 1</sup>, Seung-Hwan Lee <sup>b, \*, 1</sup>, Hyo-Jin Ahn <sup>c, \*\*, 1</sup>, Jung-Rag Yoon <sup>a, \*\*\*, 1</sup>

<sup>a</sup> R&D Center, Samwha Capacitor, South Korea

<sup>b</sup> Institute for Research in Electronics and Applied Physics, University of Maryland, College Park, MD 20742, USA

<sup>c</sup> Department of Materials Science & Engineering, Seoul National University of Science and Technology, Seoul, 01811, South Korea



## ARTICLE INFO

### Article history:

Received 8 February 2018

Received in revised form

18 March 2018

Accepted 20 March 2018

Available online 21 March 2018

### Keywords:

Granule  $\text{Li}_4\text{Ti}_5\text{O}_{12}$

Carbon nanotube

Hybrid supercapacitors

Ionic and electronic conductivity

Suppression of particle growth and

aggregation

## ABSTRACT

We prepare granule  $\text{Li}_4\text{Ti}_5\text{O}_{12}$ /carbon nanotube composite (LTO/CNT) using intermediate  $\text{Li}_2\text{TiO}_3$  and then used as an anode of hybrid supercapacitors. The hybrid supercapacitors fabricated with LTO/CNT anode with 3 wt% CNT and activated carbon (AC) cathode deliver superior electrochemical performances. It is mainly ascribed to the reduced charge-transfer resistance and improved ionic and electronic conductivity, resulting from smooth and rapid lithium ion kinetics and electron diffusion by suppression of particle growth and aggregation. Moreover, elastic properties of CNT can alleviate the volume change of LTO during charge-discharge process, resulting in excellent cycle performance. The performance improvement such as discharge capacitance, rate capability, and cyclability as well as energy and power density demonstrate that 3 wt% CNT addition in LTO anode appeal for high performance hybrid supercapacitors.

© 2018 Elsevier B.V. All rights reserved.

## 1. Introduction

Recently, the dramatically growing smart device and electric vehicle market require alternative of existing energy storage device. Because they need higher energy and power densities than traditional systems such as lithium ion batteries (LIBs) and supercapacitors to achieve high performances [1]. So far, LIBs have been widely used as energy storage devices (ESDs). Although it has a high energy density ( $\sim 200 \text{ Wh kg}^{-1}$ ), it has limitations as future ESDs due to low power density ( $50\text{--}200 \text{ W kg}^{-1}$ ) and short cycle life ( $\sim$ thousands of cycles). To complement the drawback of the LIBs, the supercapacitors, having high power density ( $\sim 3 \text{ kW kg}^{-1}$ ) and semi-permanent life time, have been used independently or coupled with LIBs. However, there is a fatal drawback of low energy density ( $20\text{--}50 \text{ Wh kg}^{-1}$ ) due to low specific capacitance of carbon based materials [2,3].

To solve these issues, hybrid supercapacitors have been designed to combine the advantages and to overcome the disadvantages of the two ESDs. The hybrid supercapacitors, generally composed of metal oxide anode derived from LIBs and AC cathode derived from supercapacitors can deliver superior energy density with excellent power density and stable cycle performances [4,5]. A study for improving the performance of a hybrid super capacitor is as follows: (i) improvement in life span and power density for battery-type anode; (ii) suppression in gas generation for high reliability; and (iii) improvement in energy density for supercapacitor-type cathode [6–9].

Among many metal oxides, spinel LTO can be regarded as a promising anode for use in ESDs because it is known as a “zero strain characteristics” due to the minute structural changes during charge-discharge process with safe operating voltage of 1.55 V (vs.  $\text{Li/Li}^+$ ). These imply that LTO enables the super long cycle life. Also, it can deliver high energy and power density compared to AC due to its 3D lithium ion diffusion in the LTO and higher theoretical capacity of  $175 \text{ mAh g}^{-1}$  [5,10], which are the three most important parameters required in ESDs. In addition, LTO is non-toxic, cheap and easy to synthesize [5].

However, among the two electrodes, as an insulator, the LTO anode causes deterioration in performance of hybrid

\* Corresponding author.

\*\* Corresponding author.

\*\*\* Corresponding author.

E-mail addresses: [shlee83@umd.edu](mailto:shlee83@umd.edu) (S.-H. Lee), [hjahn@seoultech.ac.kr](mailto:hjahn@seoultech.ac.kr) (H.-J. Ahn), [yoonyungrag@samwha.com](mailto:yoonyungrag@samwha.com) (J.-R. Yoon).

<sup>1</sup> These authors equally contributed to this work.

supercapacitors due to the inferior ionic and electronic conductivity. For ionic conductivity, it is possible to move lithium ions quickly through granules with porous microstructure. For electronic conductivity, it is the one of the effective way to form composite with conducting materials for high electronic conductivity. In this composite, the randomly distributed conducting materials within the whole composite enables remarkably rapid electron transport. The CNT has been widely used in the field of ESDs due to its superior electronic conductivity, good mechanical strength, and large-scale availability [11]. Therefore, CNT can help the LTO anode deliver excellent electrochemical performances, benefiting from the smooth and rapid electron transport by highly conductive CNT network [12]. Moreover, CNT restrain the grain growth of LTO and prevent the LTO aggregation, resulting in high electrochemical performance especially under high current density. It can be explained by superior reactivity and shorter Li ion diffusion path during charge-discharge process [13]. In addition, it was reported that production of the two-step process of synthesizing intermediate material  $\text{Li}_2\text{TiO}_3$  is an effective method to obtain final materials LTO with small grain size, key factor to affect the electrochemical performances of hybrid supercapacitors [14].

Here, we fabricated hybrid supercapacitors using LTO/CNT anode and AC cathode and investigated the effect of the CNTs contents on the electrochemical performances of hybrid supercapacitors.

## 2. Experimental

The LTO/CNT were prepared in two stage process, as shown in Fig. 1. The first stage is to prepare the granule  $\text{Li}_2\text{TiO}_3$ . The intermediate  $\text{Li}_2\text{TiO}_3$  was prepared by a conventional solid-state reaction using  $\text{Li}_2\text{CO}_3$  and anatase  $\text{TiO}_2$  with molar ratio of  $\text{Li}_2\text{CO}_3$ : $\text{TiO}_2 = 2:5$  as starting materials. For the  $\text{Li}_2\text{TiO}_3$ , the  $\text{Li}_2\text{CO}_3$  and  $\text{TiO}_2$  were mixed in ethyl alcohol for 24 h in a ball mill [15]. The slurry was spray-dried at the temperature of  $200^\circ\text{C}$  using a two-fluid nozzle with a pressure of  $3.5\text{ kg/cm}^2$ . Afterward, the granule  $\text{Li}_2\text{CO}_3/\text{TiO}_2$  was calcined at  $500^\circ\text{C}$ . The second stage is to prepare the LTO/CNT. The as-prepared  $\text{Li}_2\text{TiO}_3$  was mixed with different amounts of CNT (1, 3 and 5 wt%) and ultrasonicated for 1 h to disperse CNT in granule  $\text{Li}_2\text{TiO}_3$ . Finally, the granule  $\text{Li}_4\text{Ti}_5\text{O}_{12}/\text{CNT}$  was prepared by calcining granule  $\text{Li}_2\text{TiO}_3/\text{CNT}$  at a temperature of  $750^\circ\text{C}$  in nitrogen atmosphere to avoid the oxidation of CNT.

The hybrid supercapacitors were fabricated with LTO/CNT anode with different CNT contents and activated carbon (AC) cathode. An AC cathode was fabricated by mixing AC (MSP-20, 90 wt%) with

conductive carbon (5 wt%) and polytetrafluoroethylene (PTFE, 5 wt%). In order to prepare the anode, LTO/CNT powder, conductive carbon black binder (Super P), and polyvinylidene fluoride (PVDF) were mixed in an 83:7:10 wt ratio. N-Methyl pyrrolidinium (NMP) solvent was added to produce the slurry. This was casted on aluminum foil to a thickness of  $125\ \mu\text{m}$  and then dried at  $100^\circ\text{C}$  to remove the NMP solvent. The aluminum foil was pressed to a thickness of  $70\text{--}80\ \mu\text{m}$ . The hybrid supercapacitors were assembled with LTO/CNT as an anode and AC as a cathode in argon-gas-filled glove box. The width of the cathode, separator, and anode were 28 cm, 40 cm, and 30 cm, respectively and the heights of the cathode and anode were both 3 cm. Before being impregnated with a 1.5 M solution of  $\text{LiPF}_6$  solution in 1:1 ethylene carbonate (EC):dimethyl carbonate (DMC) as the electrolyte, in order to remove the moisture in the cell, the fabricated cell was dried in a vacuum oven for 48 h.

The thermogravimetry and differential thermal analysis (TG-DTA) were conducted by a STA-449-F3 thermal analyzer (NETZSCH). The structure properties of powders were analyzed using X-ray diffraction (XRD) and scanning electron microscopy (SEM). The electrochemical impedance spectroscopy (EIS) was conducted using a CHI660D electrochemical workstation in the frequency range of  $10^{-1}$  to  $10^3$  Hz. The initial charge-discharge capacitances, rate capabilities and cycle performances of the fabricated hybrid supercapacitors were carried out using an Arbin BT 2042 battery test system with a cut-off voltage of 1.5–2.8 V.

## 3. Results and discussion

TG-DTA provides detailed information about mechanism of the solid state reaction between  $\text{Li}_2\text{CO}_3$  and  $\text{TiO}_2$ . As shown in Fig. 2, there is a little weight loss until  $270^\circ\text{C}$  due to evaporation absorbed water. It can be clearly seen that there is a first exothermic peak appears at  $270^\circ\text{C}$  extends up to  $520^\circ\text{C}$ . It can be explained by the decomposition of  $\text{Li}_2\text{CO}_3$  and the formation of monoclinic  $\text{Li}_2\text{TiO}_3$  by reaction of  $\text{Li}_2\text{O}$  and  $\text{TiO}_2$ , which was synthesized by solid state reaction according to the following reaction [16]:



TGA curves is stationary with increasing temperature above  $520^\circ\text{C}$ , indicating  $\text{Li}_2\text{TiO}_3$  is obtained above  $520^\circ\text{C}$ . The second exothermic peak appears at  $560^\circ\text{C}$  in DTA curve reveals the

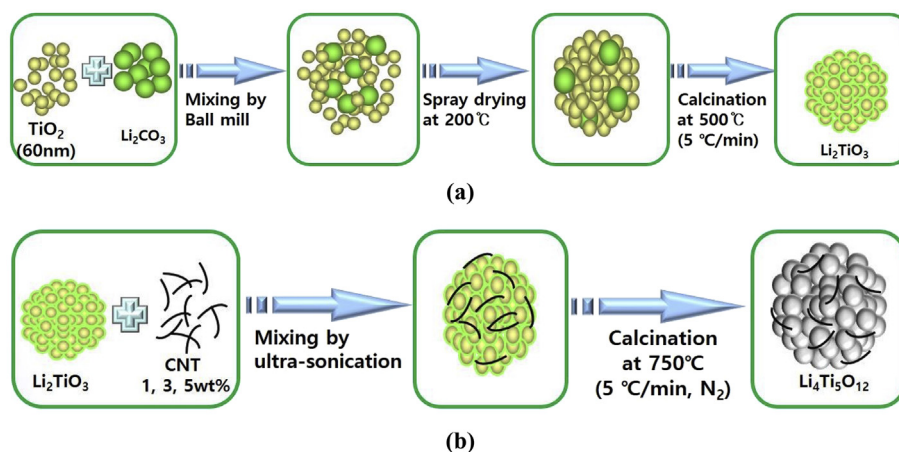


Fig. 1. Schematic illustration for the preparation procedure of the (a)  $\text{Li}_2\text{TiO}_3$  intermediate phase and (b) LTO/CNT anode materials.

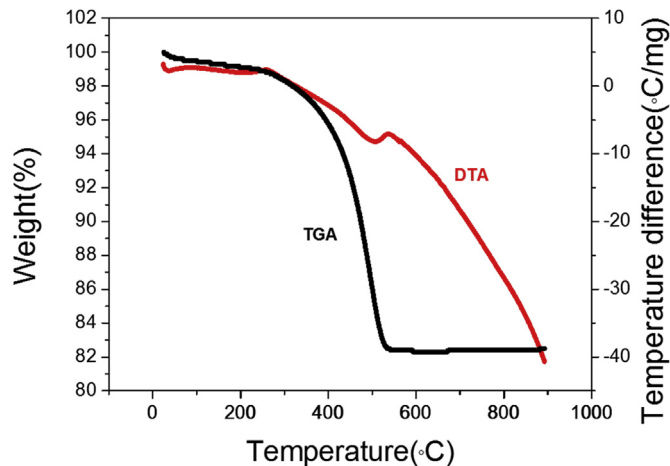


Fig. 2. TG-DTA curves of the  $\text{Li}_2\text{CO}_3$  and  $\text{TiO}_2$  powders.

transformation from  $\text{Li}_2\text{TiO}_3$  to  $\text{Li}_4\text{Ti}_5\text{O}_{12}$  without any weight loss, which can be expressed by following reaction [10]:



The formation of  $\text{Li}_4\text{Ti}_5\text{O}_{12}$  can be also achieved by the following additional reaction [17]:

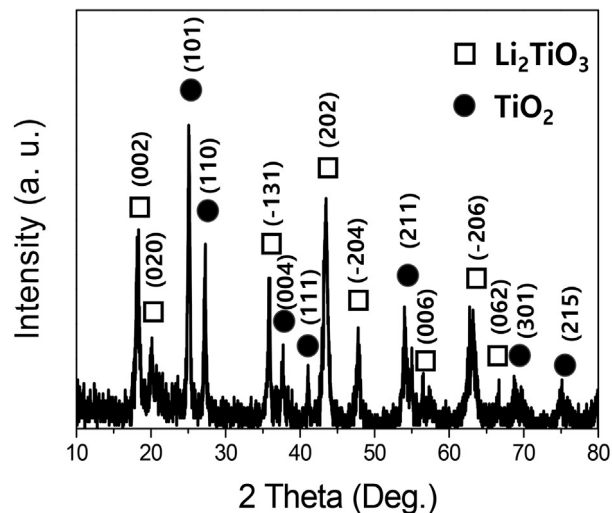


Fig. 3(a) shows the XRD pattern of stoichiometric starting mixtures of precursors ( $\text{Li}_2\text{TiO}_3$  and  $\text{TiO}_2$ ) after annealing at  $520^\circ\text{C}$ . The diffraction peak indicates that the synthesized  $\text{Li}_2\text{TiO}_3$  and unreacted  $\text{TiO}_2$  coexisted [18,19]. Also, it can be confirmed that different amount (1, 3 and 5 wt%) of CNT were well dispersed homogeneously in  $\text{Li}_2\text{TiO}_3$  (Fig. 3(b)) by ultrasonic treatment, inducing positive effect on the anode for hybrid supercapacitors.

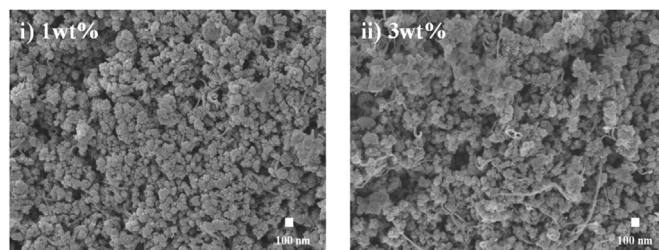
Fig. 4(a) shows the XRD patterns of the LTO after heated at  $750^\circ\text{C}$  using  $\text{Li}_2\text{TiO}_3$  with different CNT contents (1, 3 and 5 wt%). All samples were successfully synthesized into LTO regardless of CNT contents. To investigate the effect of CNT on LTO microstructure, we measured the SEM images of  $\text{Li}_4\text{Ti}_5\text{O}_{12}$  with different CNT contents, as shown in Fig. 4(b). All samples show the similar morphologies but different sizes due to CNT contents. The grain size of LTO/CNT decrease with increasing CNT content. The average particle size of 1 wt%, 3 wt% and 5 wt% shows about 330, 275 and 220 nm, respectively. The CNT is located at the grain boundaries, which inhibits the grain growth through different grain-growth retardation mechanism [18,19]. Therefore, we can conclude that CNT not only improve the conductivity of LTO but also control the particle size. This difference in particle size will affect the electrochemical performances of hybrid supercapacitors.

Fig. S1 show the cyclic voltammetry (CV) curves to investigate the electrochemical activity of hybrid supercapacitors. Fig. S1 shows the typical CV curves of hybrid supercapacitors [2]. Below 1.5 V, AC is the only electrode for charging in hybrid supercapacitors since LTO has a working voltage of more than 1.5 V. The small amount of charges occurred in this process. The charging of hybrid supercapacitors is activated at 1.5 V. Therefore, all hybrid supercapacitors have a pair of broad oxidation and reduction peaks in the range from 2.3 V to 2.5 V. The area surrounded by CV curves for the 3 wt% CNT is the largest, thus it can be inferred that the 3 wt% CNT has the better electrochemical activity. It also affects the initial charge-discharge capacitance.

Fig. 5 shows the initial discharge curve of hybrid supercapacitors



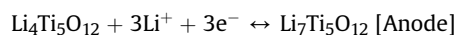
(a)



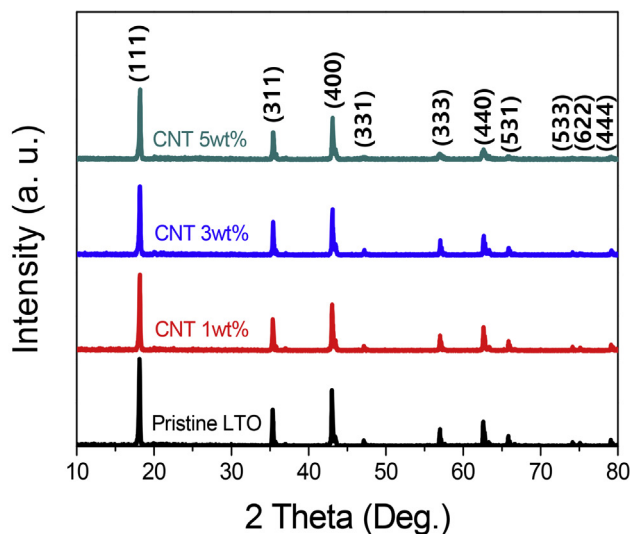
(b)

Fig. 3. (a) XRD patterns of the  $\text{Li}_2\text{TiO}_3$  (b) SEM images of the  $\text{Li}_2\text{TiO}_3$  with different CNT contents.

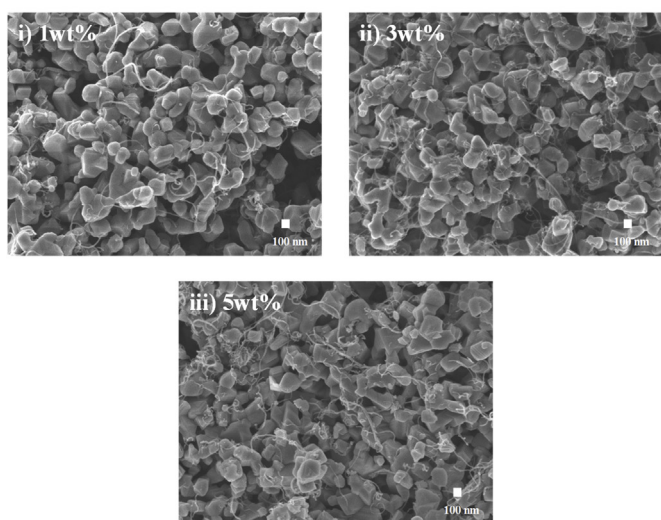
using LTO anode with various amounts of CNT contents in the voltage range of 1.5 V–2.8 V (vs  $\text{Li}/\text{Li}^+$ ) due to its cut-off voltage of 1.5 V [20]. When a hybrid supercapacitor operates outside of a cut-off voltage, decomposition of the electrolyte results in a rapid decrease in performance [21]. The two different charge storage mechanisms at the anode and cathode can be expressed by the following reactions [22]:



It can be confirmed that the LTO/CNT shows a higher discharge capacitance than that of pristine LTO, indicating superior lithium ion storage capacity. The higher capacitance can be explained by significant synergy effect of effective electron transport of CNT and rapid lithium ion intercalation of LTO. However, upon increasing the CNT content to above 3 wt%, the LTO/CNT can lead to



(a)



(b)

Fig. 4. (a) XRD patterns and (b) SEM images of the LTO with different CNT contents.

degradation of discharge capacitance by difficult dispersing and easy aggregation [23,24]. The discharge capacitance of the hybrid supercapacitors using LTO anode with various amounts of CNT contents can be calculated by following equations [25]:

$$C = \frac{q}{\Delta V \times m} = \frac{\int i \Delta t}{\Delta V \times m} \quad (6)$$

where 'C' is the capacitance ( $\text{Fg}^{-1}$ ), ' $\Delta V$ ' is the voltage change, ' $m$ ' is the mass of the active materials in both electrodes, ' $q$ ' is the total charge, ' $i$ ' is the current, and ' $t$ ' is time. The discharge capacitances of LTO/CNT (0, 1, 3 and 5 wt% CNT) are 45.5, 50.1, 56.1 and 34.1  $\text{Fg}^{-1}$ , respectively. The 3 wt% shows the highest discharge capacitance among other samples, which is also higher value than those of previously reported LTO hybrid supercapacitors [23,25,26]. The excessive CNT gradually decreased the capacitances of hybrid supercapacitors. The CNT are unable to provide high discharge capacitance due to their lack of intercalation capability with lithium

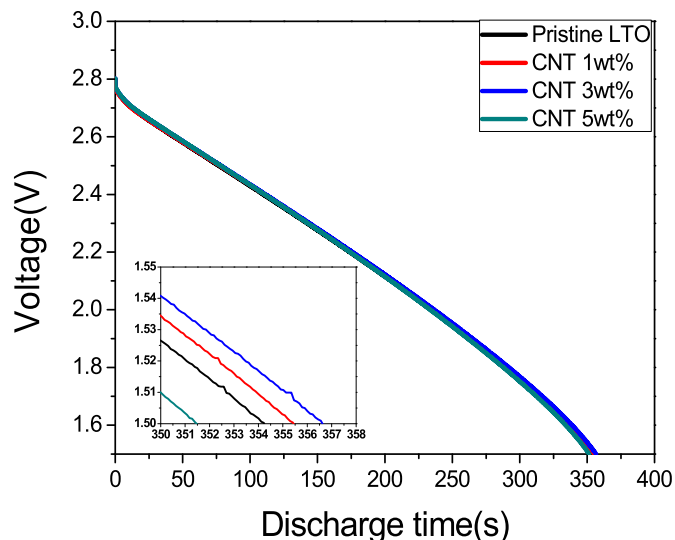


Fig. 5. Initial discharge curves of hybrid supercapacitors using LTO with different CNT contents at a current density of 1 A.

but it increases mass of active materials [10].

More importantly, there is a voltage drop in the discharge curves of hybrid supercapacitors, derived from different capacitive mechanisms, at the beginning of the discharge process. The voltage drop is generally attributed to slow lithium ion storage mechanism of anode [26]. The voltage drop can be obtained using the following relationship [27]:

$$R = \frac{V_{\text{charge}} - V_{\text{discharge}}}{2I} \quad (7)$$

' $V_{\text{charge}}$ ' is the voltage of the cell at the end charge, ' $V_{\text{discharge}}$ ' is the voltage of the cell at the starting discharge, and ' $I$ ' is the absolute value of charge and discharge current. Among others, the voltage drop of 3 wt% CNT is the smallest value of 0.025  $\Omega$ , demonstrating excellent electrical conductivity and intrinsic reversibility [28,29]. The porous structure of LTO is favorable for lithium ion accessibility to the anode and appropriate amount of CNT also provides additional electron transport pathways in addition to carbon black [30]. These structural advantages are expected to be noticeable in rate capability and long-term cycle performance due to the decrease in polarization of the hybrid supercapacitors.

Fig. 6 shows the rate capability of hybrid supercapacitors using LTO anode with various amounts of CNT contents. All retention of LTO/CNT are comparable to that of LTO at low current density of 0.5  $\text{A g}^{-1}$ . However, we observed that the difference in retention of all samples increase in proportion to the current density. Compared to LTO/CNT (1 and 3 wt%), the LTO delivers inferior rate capability under all measured current densities. The LTO shows only 69% retention especially under high current density of 6  $\text{A g}^{-1}$  of the value achieved at 0.5  $\text{A g}^{-1}$ , whereas 3 wt% CNT still maintained retention of 73% under same condition, indicating better electrochemical activity and reversibility. It can be explained by enlarged electrode/electrolyte contact surface area, resulting from small grain size, which shorten the length of lithium ions and electrons, as mentioned above. The CNT effectively prevents the grain size of LTO by strong entangled network, resulting from decrease in atomic diffusion coefficient. This is caused by the presence of CNT at the grain boundaries [18,30]. However, 5 wt% CNT shows the worst rate performance due to randomly stacked CNT.

The cyclability of hybrid supercapacitors using LTO anode with

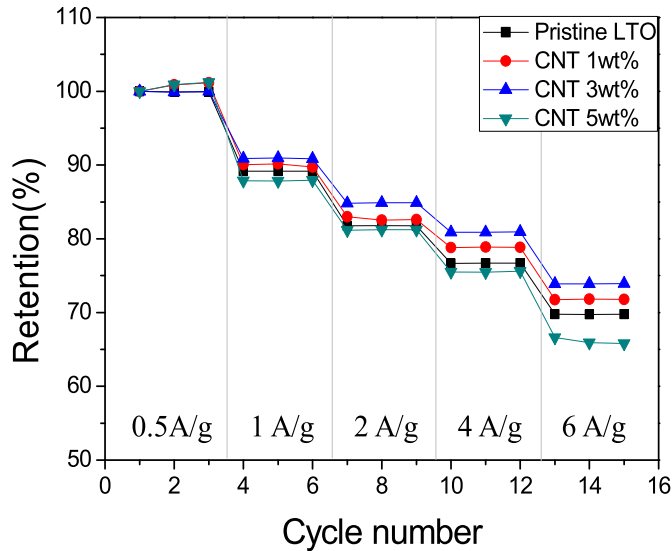


Fig. 6. Rate capabilities of hybrid supercapacitors using LTO with different CNT.

various amounts of CNT contents were conducted, as shown in Fig. 7. We can confirm that appropriate CNT addition facilitates improvement cyclability of LTO, indicating that CNT is advantageous to the stable and reversible lithium ion insertion-extraction by chemical and mechanical robustness. The 3 wt% CNT shows the capacitance retention of 92% after 6000 cycles at the current density of  $1 \text{ A g}^{-1}$ . Fig. S2 shows the XRD pattern of 3 wt% CNT after 6000 cycles. It can be confirmed that the positions of each peak for 3 wt% CNT show almost no change, indicating excellent reversibility and stability of LTO during cycling [25,31]. On the other hand, cycle efficiency of pristine LTO is only 84% after 6000 cycles. This is due to the following roles of the CNT in 3D network structure: i) CNT has high electronic conductivity and electrochemical stability, ii) it can reduce the irreversible losses of the LTO anode and improve the utilization rate and iii) it can also store lithium ions below 1 V, which is mutually beneficial since LTO stores lithium above 1.5 V [32–34]. More importantly, elastic properties of CNT can relieve the internal stress, resulting from LTO volume change of electrode during charge-discharge process, resulting in outstanding electrode stability [24,35]. The remarkable cycle performance of 3 wt% CNT is

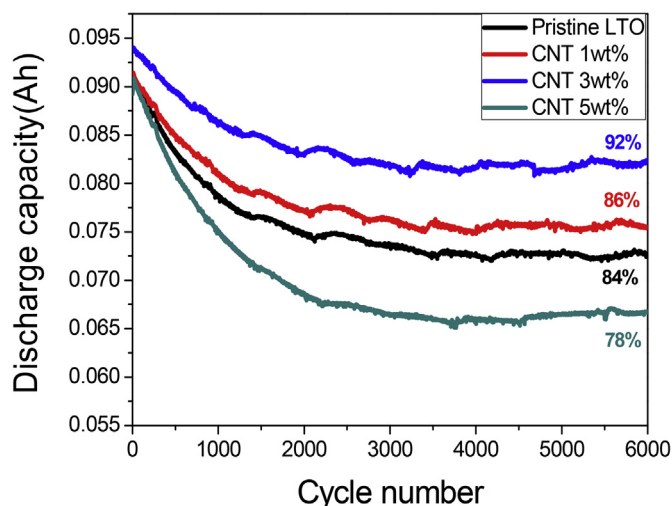


Fig. 7. Cycle performances of hybrid supercapacitors using LTO with different CNT.

very promising to meet the super long-life requirement for hybrid supercapacitors.

To better understand the excellent electrochemical performance of hybrid supercapacitors, EIS measurements were conducted. Fig. 8 shows the typical Nyquist plots of hybrid supercapacitors using LTO anode with various amounts of CNT contents. All hybrid supercapacitors show two regions, related to the electrochemical mechanism: The arc at high frequencies originated from electrolyte resistance ( $R_s$ ) and interfacial charge-transfer resistance ( $R_{ct}$ ), which is a key factor, determining the performance of hybrid supercapacitors. The straight line with a constant slope at low frequencies, referred to as a Warburg element. It represents the diffusion of lithium ion into the bulk electrode [36–38]. The semicircle indicates the charge transfer resistance ( $R_{ct}$ ) and electrolyte resistance ( $R_s$ ) at high frequency. As expected, the 3 wt% CNT exhibits the lowest  $R_{ct}$  of  $0.016 \Omega$  compared to others, indicating smaller electrochemical polarization during charge-discharge process. The low  $R_{ct}$  is attributed to the presence of appropriate CNT such as electrical percolation network and small grain size of LTO, which renders the lower  $R_{ct}$  [35]. The porous LTO enables to be well wetted by the electrolyte, thus facilitating the smooth and rapid lithium ions. Moreover, CNT not only forms continuous paths for rapid and stable electron transport but also acts as a conductive bridge in the anode, enabling the efficient insertion-extraction of lithium ions [39]. However, the excessive CNT content above 3 wt% in LTO anode leads to high  $R_{ct}$  by poor dispersion and serious aggregation of CNT [24]. It can be inferred that the combination proper amount of CNT and LTO together can significantly enhance the conductivity of CNT/LTO anode, otherwise negative effect can influence on hybrid supercapacitors.

Fig. 9 shows the Ragone plot of hybrid supercapacitors using LTO with 3 wt% CNT anode and AC cathode. The energy and power densities can be calculated by the following equations [4]:

$$P = \Delta E \times \frac{I}{m} \quad (8)$$

$$E = P \times t \quad (9)$$

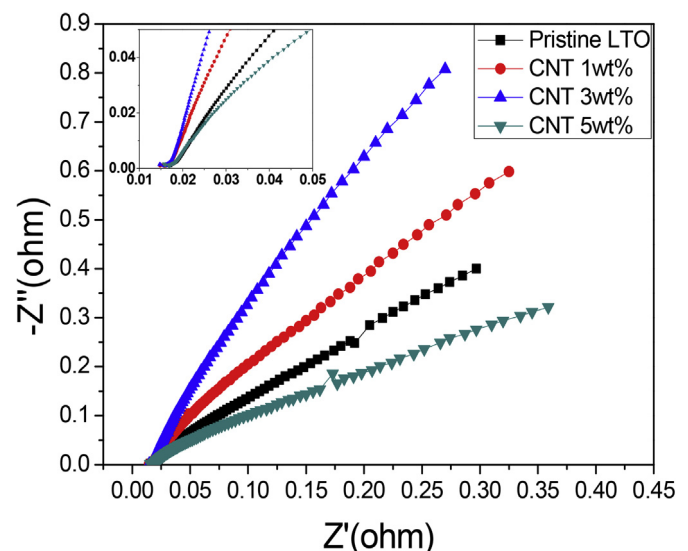


Fig. 8. EIS curves of hybrid supercapacitors using LTO with different CNT.

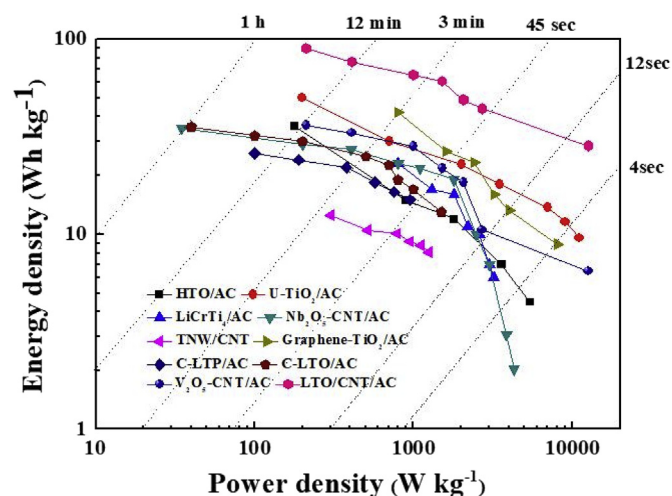


Fig. 9. Ragone plots of hybrid supercapacitors using LTO with 3 wt% CNT.

$$\Delta E = \frac{E_{max} + E_{min}}{2} \quad (10)$$

where ' $E_{max}$ ' is the potential at the starting discharge, ' $E_{min}$ ' is the potential at the end discharge, ' $I$ ' is the charge and discharge currents, ' $m$ ' is the mass of active materials including the anode and cathode electrodes, and ' $t$ ' is the discharge time in the hybrid supercapacitor. The energy and power densities of LTO with 3 wt% CNT anode and AC cathode hybrid supercapacitors ranged from 22.4 to 84.2 Wh kg<sup>-1</sup> and from 195.4 to 12652.5 W kg<sup>-1</sup>, respectively. These remarkable values also meet the requirement of hybrid electric vehicle (HEV) application. The hybrid supercapacitors using LTO with 3 wt% CNT anode show superior energy and power densities compared to other hybrid supercapacitors such as TiO<sub>2</sub>-(reduced graphene oxide)/AC [40], TiO<sub>2</sub>-(B) nanowire (TNW)/carbon nanotubes (CNTs) [41], C-Li<sub>4</sub>Ti<sub>5</sub>O<sub>12</sub> (LTO)/AC [42], C-LiTi<sub>2</sub>(PO<sub>4</sub>)<sub>3</sub> (LTP)/AC [43], V<sub>2</sub>O<sub>5</sub>-CNT/AC [44], Nb<sub>2</sub>O<sub>5</sub>-CNT/AC [45], H<sub>2</sub>Ti<sub>12</sub>O<sub>25</sub>-AC [2], LiCrTi<sub>4</sub>/AC [46], and urchin-like TiO<sub>2</sub>/AC [47]. Therefore, we can infer that LTO with 3 wt% CNT anode is a practical way to improve the energy and power density for hybrid supercapacitors.

#### 4. Conclusion

We fabricated hybrid supercapacitors using LTO/CNT anode with different contents of CNT and AC cathode. By adding appropriate CNT contents to LTO anode, the outstanding electrochemical performances of hybrid supercapacitors can be achieved, indicating the practical applicability of the LTO/CNT anode. The 3 wt% CNT delivered not only a high discharge capacitance of 56.1 F g<sup>-1</sup>, but also an excellent rate capability (73% even at a high current density of 6 A g<sup>-1</sup>) and ultra-long cycle life (92% after 6000 cycles). Moreover, the energy density of 22.4 and 84.2 Wh kg<sup>-1</sup> are attained at power density of 12652.5 and 195.4 W kg<sup>-1</sup>, respectively. It can be elucidated by the synergy effect of CNT on the grain growth inhibition, high electronic and ionic conductivity, enabling superior electrochemical performances. We therefore reach the conclusion that the addition of 3 wt% CNT in the LTO anode is very promising anode for high performance hybrid supercapacitors.

#### Acknowledgments

This work was supported by the Industrial Fundamental

Technology Development Program (10080656, Development of ceramic/carbon convergence and integration anode material for 10C fast charging Lithium ion battery) funded by the Ministry of Trade, Industry and Energy of Korea.

#### Appendix A. Supplementary data

Supplementary data related to this article can be found at <https://doi.org/10.1016/j.jallcom.2018.03.248>.

#### References

- [1] G.H. An, D.Y. Lee, Y.J. Lee, H.J. Ahn, Ultrafast lithium storage using antimony-doped tin oxide nanoparticles sandwiched between carbon nanofibers and a carbon skin, *ACS Appl. Mater. Interfaces* 8 (2016) 30264–30270.
- [2] J.H. Lee, H.K. Kim, E. Baek, M. Pecht, S.H. Lee, Y.H. Lee, Improved performance of cylindrical hybrid supercapacitor using activated carbon/niobium doped hydrogen titanate, *J. Power Sources* 301 (2016) 348–354.
- [3] G.H. An, D.Y. Lee, H.J. Ahn, Carbon-encapsulated hollow porous vanadium-oxide nanofibers for improved lithium storage properties, *ACS Appl. Mater. Interfaces* 8 (2016) 19466–19474.
- [4] J.H. Kim, H.J. Choi, H.K. Kim, S.H. Lee, Y.H. Lee, A hybrid supercapacitor fabricated with an activated carbon as cathode and an urchin-like TiO<sub>2</sub> as anode, *Int. J. Hydrogen Energy* 41 (2016) 13549–13556.
- [5] B.G. Lee, S.H. Lee, Application of hybrid supercapacitor using granule Li<sub>4</sub>Ti<sub>5</sub>O<sub>12</sub>/activated carbon with variation of current density, *J. Power Sources* 343 (2017) 545–549.
- [6] R. Yi, S. Chen, J. Song, M.L. Gordin, A. Manivannan, High-performance hybrid supercapacitor enabled by a high-rate Si-based anode, *Adv. Funct. Mater.* 24 (2014) 7433–7439.
- [7] S.H. Lee, S.G. Lee, J.R. Yoon, H.K. Kim, Novel performance of ultrathin AlPO<sub>4</sub> coated H<sub>2</sub>Ti<sub>12</sub>O<sub>25</sub> Exceeding Li<sub>4</sub>Ti<sub>5</sub>O<sub>12</sub> in cylindrical hybrid supercapacitor, *J. Power Sources* 273 (2015) 839–843.
- [8] Y.B. He, B. Li, M. Liu, C. Zhang, W. Lv, C. Yang, J. Li, H. Du, B. Zhang, Q.H. Yang, J.K. Kim, F. Kang, Gassing in Li<sub>4</sub>Ti<sub>5</sub>O<sub>12</sub>-based batteries and its remedy, *Sci. Rep.* 2 (2012) 913.
- [9] K. Sheng, Y. Sun, C. Li, W. Yuan, G. Shi, Ultrahigh-rate supercapacitors based on electrochemically reduced graphene oxide for ac line-filtering, *Sci. Rep.* 2 (2012) 247.
- [10] R. Qing, L. Liu, H. Kim, W.M. Sigmund, Electrochemical property dependence of electrochemical performance for TiO<sub>2</sub>/CNT core-shell nanofibers in lithium ion batteries, *Electrochim. Acta* 180 (2015) 295–306.
- [11] B. Wang, H. Xin, X. Li, J. Cheng, G. Yang, F. Nie, Mesoporous CNT@TiO<sub>2</sub>-C nanocable with extremely durable high rate capability for lithium-ion battery anodes, *Sci. Rep.* 4 (2014) 1–7.
- [12] W. Zuo, R. Li, C. Zhou, Y. Li, J. Xia, J. Liu, Battery-supercapacitor hybrid devices: recent progress and future prospects, *Adv. Sci.* 4 (2017), 16005391–1600545.
- [13] L. Wang, H. Zhang, Q. Deng, Z. Huang, A. Zhou, J. Li, Superior rate performance of Li<sub>4</sub>Ti<sub>5</sub>O<sub>12</sub>/TiO<sub>2</sub>/C/CNTs composites via microemulsion-assisted method as anodes for lithium ion battery, *Electrochim. Acta* 142 (2014) 202–207.
- [14] E. Matsui, Y. Abe, M. Senna, Solid-state synthesis of 70 nm Li<sub>4</sub>Ti<sub>5</sub>O<sub>12</sub> particles by mechanically activating intermediates with amino acids, *J. Am. Ceram. Soc.* 91 (2008) 1522–1528.
- [15] C.L. Huang, Y.W. Tseng, J.Y. Chen, High-Q dielectrics using ZnO-modified Li<sub>2</sub>TiO<sub>3</sub> ceramics for microwave applications, *J. Eur. Ceram. Soc.* 32 (2012) 3287–3295.
- [16] Y.Z. Hao, H. Yang, G.H. Chen, Q.L. Zhang, Microwave dielectric properties of Li<sub>2</sub>TiO<sub>3</sub> ceramics doped with LiF for LTCC applications, *J. Alloy. Comp.* 552 (2013) 173–179.
- [17] H. Kaftlen, M. Tuncer, S. Tu, S. Repp, H. Göcmez, R. Thomann, S. Weber, E. Erdem, Mn-substituted spinel Li<sub>4</sub>Ti<sub>5</sub>O<sub>12</sub> materials studied by multifrequency EPR spectroscopy, *J. Mater. Chem.* 1 (2013) 9973–9982.
- [18] F. Inam, H. Yan, T. Peijs, M.J. Reece, The sintering and grain growth behaviour of ceramic-carbon nanotube Nanocomposites, *Compos. Sci. Technol.* 70 (2010) 947–952.
- [19] V.H. Nguyen, H.B. Gu, Synthesis and characterization of silver vanadium oxide as a cathode for lithium ion batteries, *Trans. Electr. Electron. Mater.* 17 (2016) 139–142.
- [20] B.G. Lee, S.H. Lee, J.R. Yoon, H.J. Ahn, Formation of holes into granule Li<sub>4</sub>Ti<sub>5</sub>O<sub>12</sub> anode for enhanced performance of hybrid supercapacitors, *Electrochim. Acta* 263 (2018) 555–560.
- [21] K.S. Ryu, K.M. Kim, N.G. Park, Y.J. Park, S.H. Chang, Symmetric redox supercapacitor with conducting polyaniline electrodes, *J. Power Sources* 103 (2003) 305–309.
- [22] H.K. Kim, S.H. Lee, Enhanced electrochemical performances of cylindrical hybrid supercapacitors using activated carbon/Li<sub>4-x</sub>M<sub>x</sub>Ti<sub>5-y</sub>N<sub>y</sub>O<sub>12</sub> (M = Na, N = V, Mn) electrodes, *Inside Energy* 109 (2016) 506–511.
- [23] J.H. Kim, J.R. Yoon, S.H. Lee, High tunability and performance of cylindrical hybrid supercapacitors with binary H<sub>2</sub>Ti<sub>12</sub>O<sub>25</sub>-Li<sub>4</sub>Ti<sub>5</sub>O<sub>12</sub> anodes, *Electrochim. Acta* 220 (2016) 231–236.
- [24] H. Zhang, Y. Chen, J. Li, C. He, Y. Chen, Li<sub>4</sub>Ti<sub>5</sub>O<sub>12</sub>/CNTs composite anode

- material for large capacity and high-rate lithium ion batteries, *Int. J. Hydrogen Energy* 39 (2014) 16096–16102.
- [25] J.H. Lee, S.H. Lee, Applications of novel carbon/AlPO<sub>4</sub> hybrid-coated H<sub>2</sub>Ti<sub>12</sub>O<sub>25</sub> as a high-performance anode for cylindrical hybrid supercapacitors, *ACS Appl. Mater. Interfaces* 8 (2016) 28974–28981.
- [26] H.J. Choi, S.H. Lee, J.H. Kim, H.K. Kim, J.M. Kim, Zinc doped H<sub>2</sub>Ti<sub>12</sub>O<sub>25</sub> anode and activated carbon cathode for hybrid supercapacitor with superior performance, *Electrochim. Acta* 251 (2017) 613.
- [27] J.H. Kim, S.H. Lee, Use of carbon and AlPO<sub>4</sub> dual coating on H<sub>2</sub>Ti<sub>12</sub>O<sub>25</sub> anode for high stability hybrid supercapacitor, *J. Power Sources* 331 (2016) 1–9.
- [28] Q. Huang, J. Yang, C.B. Ng, C. Jia, Q. Wang, A redox flow lithium battery based on the redox targeting reactions between LiFePO<sub>4</sub> and iodide, *Energy Environ. Sci.* 9 (2016) 917–921.
- [29] T.C. Chou, R.A. Doong, C.C. Hu, B. Zhang, D.S. Su, Hierarchically porous carbon with manganese oxides as highly efficient electrode for asymmetric supercapacitors, *ChemSusChem* 7 (2014) 841–847.
- [30] W. Deng, A. Hu, X. Chen, S. Zhang, Q. Tang, Z. Liu, B. Fan, K. Xiao, Sulfur-impregnated 3D hierarchical porous nitrogen-doped aligned carbon nanotubes as high-performance cathode for lithium-sulfur batteries, *J. Power Sources* 322 (2016) 138–146.
- [31] R. Wang, X. Lu, L. Hao, W. Jiao, W. Liu, J. Zhang, F. Yuan, F. Yang, Enhanced and tunable photochromism of MoO<sub>3</sub>-butylamine organic-inorganic hybrid composites, *J. Mater. Chem. C* 5 (2017) 427–433.
- [32] F.F. Cao, Y.G. Guo, S.F. Zheng, X.L. Wu, L.Y. Jiang, R.R. Bi, L.J. Wan, J. Maiser, Symbiotic coaxial nanocables: facile synthesis and an efficient and elegant morphological solution to the lithium storage problem, *Chem. Mater.* 22 (2010) 1908–1914.
- [33] Y.H. Chen, C.W. Wang, X. Zhang, A.M. Sastry, Porous cathode optimization for lithium cells: ionic and electronic conductivity, capacity, and selection of materials, *J. Power Sources* 195 (2010) 2851–2862.
- [34] X. Jianrong, Z. Hang, J. Aihua, W. Hongzhe, L. Yanwei, Preparation and lithium storage properties of active carbon-CNT/sulfur composite, *Ionics* 21 (2015) 1241–1246.
- [35] Y.R. Zhu, P. Wang, T.F. Yi, L. Deng, Y. Xie, Improved high-rate performance of Li<sub>4</sub>Ti<sub>5</sub>O<sub>12</sub>/carbon nanotube nanocomposite anode for lithium-ion batteries, *Solid State Ionics* 276 (2015) 84–89.
- [36] J. Xu, C.C. Mi, B. Cao, J. Cao, A new method to estimate the state of charge of lithium-ion batteries based on the battery impedance model, *J. Power Sources* 233 (2013) 277–284.
- [37] W. Wang, S. Guo, L. Lee, K. Ahmed, J. Zhong, Z. Favors, F. Zaera, M. Ozkan, C.S. Ozkan, Hydrous ruthenium oxide nanoparticles anchored to graphene and carbon nanotube hybrid foam for supercapacitors, *Sci. Rep.* 4 (2014) 4452.
- [38] J.R. Yoon, E. Baek, H.K. Kim, M. Pecht, S.H. Lee, Critical dual roles of carbon coating in H<sub>2</sub>Ti<sub>12</sub>O<sub>25</sub> for cylindrical hybrid Supercapacitors, *Carbon* 101 (2016) 9–15.
- [39] H. Wang, G. Jia, Y. Guo, Y. Zhang, H. Geng, J. Xu, W. Mai, Q. Yan, H.J. Fan, Atomic layer deposition of amorphous TiO<sub>2</sub> on carbon nanotube networks and their superior Li and Na ion storage properties, *Adv. Mater. Interfaces* 3 (2016) 1600375–1600383.
- [40] H. Kim, M.Y. Cho, M.H. Kim, K.Y. Park, H. Gwon, Y. Lee, K.C. Roh, K. Kang, A novel high-energy hybrid supercapacitor with an anatase TiO<sub>2</sub>-reduced graphene oxide anode and an activated carbon cathode, *Adv. Energy Mater* 3 (2013) 1500–1506.
- [41] Q. Wang, Z.H. Wen, J.H. Li, A hybrid supercapacitor fabricated with a carbon nanotube cathode and a TiO<sub>2</sub>-B nanowire anode, *Adv. Funct. Mater.* 16 (2006), 16 2141–2216 2146.
- [42] H.G. Jung, N. Venugopal, B. Scrosati, Y.K. Sun, A high energy and power density hybrid supercapacitor based on an advanced carbon-coated Li<sub>4</sub>Ti<sub>5</sub>O<sub>12</sub> electrode, *J. Power Sources* 221 (2013) 266–271.
- [43] V. Aravindan, W. Chuiling, M.V. Reddy, G.V.S. Rao, B.V.R. Chowdari, S. Madhavi, Carbon coated nano-LiTi<sub>2</sub>(PO<sub>4</sub>)<sub>3</sub> electrodes for non-aqueous hybrid supercapacitors, *Phys. Chem. Chem. Phys.* 14 (2012) 5808–5814.
- [44] V. Aravindan, Y.L. Cheah, W.F. Mak, G. Wee, B.V.R. Chowdari, S. Madhavi, Fabrication of high energy-density hybrid supercapacitors using electrospun V<sub>2</sub>O<sub>5</sub> nanofibers with a self-supported carbon nanotube network, *Chem-PlusChem* 77 (2012) 570–575.
- [45] X. Wang, G. Li, Z. Chen, V. Augustyn, X. Ma, G. Wang, B. Dunn, Y. Lu, High-performance supercapacitors based on nanocomposites of Nb<sub>2</sub>O<sub>5</sub> nanocrystals and CarbonNanotubes, *Adv. Energy Mater.* 1 (2011) 1089–1093.
- [46] V. Aravindan, W. Chuiling, S. Madhavi, High power lithium-ion hybrid electrochemical capacitors using spinel LiCrTiO<sub>4</sub> as insertion electrode, *J. Mater. Chem.* 22 (2012) 16026–16031.
- [47] H.J. Choi, J.H. Kim, H.K. Kim, S.H. Lee, Y.H. Lee, Improving the electrochemical performance of hybrid supercapacitor using well-organized urchin-like TiO<sub>2</sub> and activated carbon, *Electrochim. Acta* 208 (2016) 202–210.